Articles

Anisometric Cyclometalated Palladium(II) and Platinum(II) Complexes. Structural and Photophysical Studies

Francesco Neve* and Alessandra Crispini

Dipartimento di Chimica, Università della Calabria, I-87030 Arcavacata di Rende (CS), Italy

Sebastiano Campagna*

Dipartimento di Chimica Inorganica, Chimica Analitica e Chimica Fisica, Università di Messina, via Sperone 31, I-98166 Messina, Italy

Received March 27, 1997[⊗]

The potentially tridentate ligand 4′-[4-(dodecyloxy)phenyl]-6′-phenyl-2,2′-bipyridine (HL^1) easily undergoes metalation at the ortho-C atom, yielding the rodlike complexes $[Pd(L^1)Cl]$ (**1**) and $[Pt(L^1)Cl]$ (**2**). The solid state features and the photophysical properties of the complexes have been studied. Crystal data for **2**: $PtC_{34}H_{39}ClN_2O$, triclinic, $P\bar{1}$, $a = 9.043(2)$ Å, $b = 10.874(2)$ Å, $c = 15.710(4)$ Å, $\alpha = 96.95(2)°$, $\beta = 92.51(2)°$, $\gamma = 102.32(2)°$, $V = 1494.3(6)$ Å^3, $Z = 2$, and final $R = 0.0387$ ($R_w = 0.0335$) for 4333 independent reflections. The electronic spectra of complexes **1** and **2** show intense absorption bands in the UV region due to metal-perturbed ligand-centered (LC) transitions. In addition, complex **2** shows a moderately intense metal-to-ligand charge-transfer (MLCT) band in the visible region. Both complexes **1** and **2** show luminescence, although under different conditions. Strong emission has been observed for a 77 K glassy solution (highest energy feature 495 nm; $\tau = 74$ μs) or room-temperature crystal ($\lambda_{max} = 490$ nm) of **1**. In both cases, the emission was assigned to a triplet LC excited state. Complex **2** exhibits emission from a ^{3}MLCT level both in solution at room temperature ($\lambda_{max} = 590$ nm; $\tau = 700$ ns; $\Phi = 0.037$) and in glass at 77 K ($\lambda_{max} = 545$ nm; $\tau = 18$ μs). The room-temperature emission of crystalline **2** (highest energy feature 590 nm) is also similar in energy to that observed in fluid solution and exhibits the typical MLCT vibrational progression, thus ruling out a contribution from either metal−metal or strong $\pi-\pi$ interactions.

Introduction

Low-dimensional supramolecular structures are highly desirable when materials with anisotropic physical properties are designed. A classical example of such a material is a one-dimensional metal showing either loose or strong metal−metal interactions in the solid state.[1] A more recent approach, in the direction of shape anisotropism, is the construction of conjugated metallopolymers,[2] molecular[3a] or supramolecular[3b,c] wires, and channels.[3b,c] On the other hand, when the focus is on the fruitful compromise between low-dimensionality and disorder the archetype would certainly be a columnar liquid crystal.[4]

For many years some of us have been involved in the synthesis of new types of thermotropic liquid crystals based on transition metals.[5] Rodlike, anisotropic molecular shapes are nearly ideal for obtaining 1-D nematic and 2-D smectic mesogenic assemblies. The above prerequisite can be satisfied when the metal is located either in the middle or at the end of a promesogenic structure.[6] A further condition to be realized is the absence of strong axial intermolecular interactions in the mesophase.

Here we describe the synthesis of the anisometric cyclometalated Pd(II) and Pt(II) derivatives of 4′-[4-(dodecyloxy)-phenyl]-6′-phenyl-2,2′-bipyridine (HL^1) (Scheme 1), a ligand able to supply a C,N,N planar donor set.[7,8] Although stacking (driven mainly by $\pi-\pi$ interactions) was foreseen,[9,10] the mismatch between planar cores and hydrocarbon chains was expected to be high and full of possibly interesting consequences.

[⊗] Abstract published in *Advance ACS Abstracts,* November 1, 1997.

(1) (a) Miller, J. S., Ed. *Extended Linear Chain Compounds*; Plenum Press: New York, 1982. (b) Keller, H. J., Ed. *Chemistry and Physics of One Dimensional Metals*; Plenum Press: New York, 1977.

(2) For recent examples, see: (a) Irwin, M. J.; Jia, G.; Vittal, J. J.; Puddephatt, R. J. *Organometallics* **1996**, *15*, 5321. (b) James, S. L.; Verspui, G.; Spek, A. L.; van Koten, G. *Chem. Commun.* **1996**, 1309. (c) Altmann, M.; Bunz, U. H. F. *Angew. Chem., Int. Ed. Engl.* **1995**, *34*, 569. (d) Jia, G.; Puddephatt, R. J.; Scott, J. D.; Vittal, J. J. *Organometallics* **1993**, *12*, 3565.

(3) (a) Harriman, A.; Ziessel, R. *Chem. Commun.* **1996**, 1707. (b) van Nostrum, C. F.; Nolte, R. J. M. *Chem. Commun.* **1996**, 2385. (c) Lehn, J. M. *Supramolecular Chemistry: Concepts and Perspectives*; VCH: Weinheim, Germany, 1995; Chapter 8.

(4) (a) Chandrasekkar, S. *Liquid Crystals*, 2nd ed.; Cambridge University Press: Cambridge, U.K., 1992; Chapter 6. (b) Vogtle, F. *Supramolecular Chemistry*; Wiley: Chichester, U.K., 1991; Chapter 8.

(5) (a) Neve, F. *Adv. Mater.* **1996**, *8*, 277. (b) Neve, F.; Ghedini, M.; De Munno, G.; Levelut, A.-M. *Chem. Mater.* **1995**, *7*, 688. (c) Neve, F.; Ghedini, M.; Levelut, A.-M.; Francescangeli, O. *Chem. Mater.* **1994**, *6*, 70. (d) Ghedini, M.; Pucci, D.; De Munno, G.; Viterbo, D.; Neve, F.; Armentano, S. *Chem. Mater.*, **1991**, *3*, 65. (e) Ghedini, M.; Armentano, S.; Neve, F.; Licoccia, S. *J. Chem. Soc., Dalton Trans.* **1988**, 1565.

(6) Serrano, J. L., Ed. *Metallomesogens*; VCH: Weinheim, Germany, 1996.

(7) (a) Bardwell, D. A.; Cargill Thompson, A. M. W.; Jeffery, J. C.; McCleverty, J. A.; Ward, M. D. *J. Chem. Soc., Dalton Trans.* **1996**, 873. (b) Constable, E. C.; Cargill Thompson, A. M. W.; Cherryman, J.; Liddiment, T. *Inorg. Chim. Acta* **1995**, *235*, 165. (c) Constable, E. C.; Henney, R. P. G.; Raithby, P. R.; Sousa, L. R. *Angew. Chem., Int. Ed. Engl.* **1991**, *30*, 1363. (d) Constable, E. C.; Henney, R. P. G.; Leese, T. A.; Tocher, D. A. *J. Chem. Soc., Dalton Trans.* **1990**, 443.

S0020-1669(97)00354-6 CCC: $14.00

Scheme 1

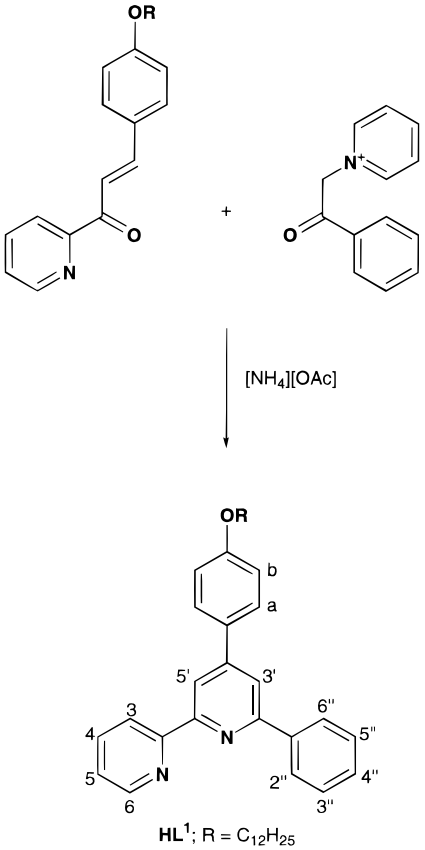

Another important aspect to be tested was the potential luminescence of the cyclometalated complexes[11] and its relevance to the preparation of new materials. The present study confirmed the ability of such systems to act as luminophores, also allowing a comparison between homologous Pd(II) and Pt(II) species. Unfortunately, a phenyl-*p*-dodecyloxy promesogenic group attached to the 6′-phenyl-2,2′-bipyridine backbone did not prove adequate to generate calamitic (based on rodlike species) mesophases from these dagger-shaped molecules. Different substituents seem to show a higher propensity to reach this goal.[12] A report on part of this work was recently communicated.[12]

Experimental Section

Materials. 2-Acetylpyridine (Aldrich), 4-(dodecyloxy)benzaldehyde (Aldrich), ammonium acetate (Lancaster), and 1-(2-oxo-2-phenylethyl)-pyridinium bromide (Lancaster) were used as received; K_2PtCl_4 was purchased from Johnson Matthey. $[Pd(PhCN)_2Cl_2]$[13] was prepared according to the literature.

Preparations. 1-(2-Pyridyl)-3-[4-(dodecyloxy)phenyl]propen-1-one. A solution of 2-acetylpyridine (639 mg, 5.27 mmol) in EtOH (10 mL) was added dropwise over 10 min to a stirred emulsion of 4-(dodecyloxy)benzaldehyde (1.532 g, 5.27 mmol) and NaOH (287 mg, 7.17 mmol) in EtOH/H_2O (40 mL; 3:1, v/v). After 24 h of stirring at room temperature, the resulting pale yellow solid was filtered off, washed with diethyl ether, and dried *in vacuo*. Yield: 94%. IR (Nujol mull): ν(CO), 1673 cm^{-1}. ^1H NMR ($CDCl_3$): δ (ppm) 8.73 (br d, 1H, pyridyl H^6), 8.18 (d, 1H, pyridyl H^3), 8.17 (d, 1H, olefinic H), 7.91 (d, 1H, olefinic H), 7.86 (br t, 1H, pyridyl H^4), 7.68 (d, 2H, phenyl $H^{2,6}$), 7.47 (m, 1H, pyridyl H^5), 6.91 (d, 2H, phenyl $H^{3,5}$), 3.99 (t, 2H, OCH_2), 1.79 (m, 2H, OCH_2CH_2), 1.45−1.26 (m, 18H, $(CH_2)_9$), 0.87 (t, 3H, CH_3).

4′-[4-(Dodecyloxy)phenyl]-6′-phenyl-2,2′-bipyridine (HL^1). A mixture of 1-(2-pyridyl)-3-[4-(dodecyloxy)phenyl]propen-1-one (800 mg, 2.03 mmol), 1-(2-oxo-2-phenylethyl)pyridinium bromide (565 mg, 2.03 mmol), and ammonium acetate (1.54 g, 20 mmol) in methanol (16 mL) was heated to reflux with vigorous stirring. The resulting orange solution turned dark green after 7 h. Overnight cooling to room temperature yielded a grayish-violet precipitate. The solid was filtered off, washed with a small amount of methanol, and dried *in vacuo*. The crude product was purified by column cromatography on SiO_2 using two different eluents consecutively. A yellow band was eluted first with CH_2Cl_2, and the yellow eluate was discarded. Further elution of a brown band with diethyl ether allowed the product to be recovered. The analytically pure product was obtained as a pinkish-brown solid upon removal of the solvent under reduced pressure. Yield: 43%. Mp: 86.5 °C. Anal. Calcd for $C_{34}H_{40}N_2O$: C, 82.88; H, 8.18; N, 5.69. Found: C, 83.01; H, 8.40; N, 5.53. ^1H NMR ($CDCl_3$): δ (ppm) 8.71 (br d, 1H, H^6), 8.68 (d, 1H, H^3), 8.60 (d, 1H, $H^{3'}$), 8.21 (d, 2H, $H^{2'',6''}$), 7.95 (d, 1H, $H^{5'}$), 7.86 (ddd, 1 H, H^4), 7.78 (d, 2 H, H^a), 7.50 (m, 3 H, $H^{3'',4'',5''}$), 7.34 (m, 1 H, H^5), 7.02 (d, 2 H, H^b), 4.02 (t, 2 H, OCH_2), 1.82 (m, 2 H, OCH_2CH_2), 1.48−1.21 (m, 18H, $(CH_2)_9$), 0.87 (t, 3H, CH_3). $^{13}C\{^1H\}$ NMR ($CDCl_3$): δ (ppm) 160.2, 157.1, 156.2, 149.8, 149.0, 139.7, 136.7, 130.9, 128.9, 128.7, 128.4, 127.1, 123.6, 121.5, 117.9, 116.9, 115.1, 68.2, 31.9, 29.6, 29.4, 29.3, 26.1, 22.7, 14.1.

[Pd(L^1)Cl] (1). A solution of $[Pd(PhCN)_2Cl_2]$ (55 mg, 0.142 mmol) in benzene (5 mL) was added to a suspension of HL^1 (70 mg, 0.142 mmol) in MeOH (5 mL). The mixture was then stirred at room temperature for 3 h, affording a pale green microcrystalline precipitate. The solid was filtered off, washed with MeOH and diethyl ether, and dried *in vacuo*. Yield: 84%. Mp: 188 °C (DSC). Anal. Calcd for $C_{34}H_{39}ClN_2OPd$: C, 64.45; H, 6.20; N, 4.40. Found: C, 64.80; H, 6.34; N, 4.05. ^1H NMR ($CDCl_3$): δ (ppm) 8.24 (br d, 1 H, H^6), 7.89 (d, 1 H, H^3), 7.75 (ddd, 1 H, H^4), 7.58 (d, 2H, H^a), 7.54 (s, 1 H, $H^{3'}$), 7.36 (d, 1 H, $H^{3''}$ or $H^{6''}$), 7.18 (s, 1 H, $H^{5'}$), 7.08 (m, 2 H, H^5 + $H^{6''}$ or $H^{3''}$), 6.97 (d, 2 H, H^b), 6.86 (br t, 1 H, $H^{4''}$ or $H^{5''}$), 6.75 (br t, 1 H, $H^{5''}$ or $H^{4''}$), 4.04 (t, 2 H, OCH_2), 1.85 (m, 2 H, OCH_2CH_2), 1.52−1.29 (m, 18 H, $(CH_2)_9$), 0.90 (t, 3 H, CH_3).

[Pt(L^1)Cl] (2). A solution of K_2PtCl_4 (100 mg, 0.24 mmol) in water (6 mL) was added to a suspension of HL^1 (120 mg, 0.24 mmol) in MeCN/EtOH (12 mL; 2:1, v/v). The mixture was heated to reflux for 20 h and then cooled. The brownish solid was removed by filtration and washed with EtOH. Further washing with diethyl ether removed a brown soluble impurity, leaving the product as a microcrystalline orange solid on the frit. Yield: 83%. Mp: 184 °C (DSC). Anal. Calcd for $C_{34}H_{39}ClN_2OPt$: C, 56.54; H, 5.44; N, 3.88. Found: C, 56.58; H, 5.50; N, 4.44. ^1H NMR ($CDCl_3$): δ (ppm) 8.59 (br d, 1H, H^6), 7.86−7.77 (m, 2 H, $H^{3,4}$), 7.58 (d, 2 H, H^a), 7.43 (br s, 1H, $H^{3'}$), 7.40 (m, 1H, $H^{3''}$ or $H^{6''}$), 7.26 (m, 1 H, H^5), 7.17 (br s, 1H, $H^{5'}$), 7.09 (m, 1H, $H^{6''}$or $H^{3''}$), 6.98 (d, 2 H, H^b) 4.04 (t, 2 H, OCH_2), 1.85 (m, 2 H, OCH_2CH_2), 1.51−1.24 (m, 18H, $(CH_2)_9$), 0.89 (t, 3H, CH_3).

Spectroscopic Characterization. Absorption spectra were recorded on a Kontron Uvikon 860 spectrophotometer. A Perkin-Elmer LS-5B spectrofluorimeter equipped with a Hamamatsu R928 phototube was used to obtain luminescence spectra. The spectra were corrected for photomultiplier response by using a standard lamp. Luminescence lifetimes were measured with an Edinburgh FL900 single-photon-counting spectrometer, using a nitrogen discharge as the pulsed-light source (pulse width: 3 ns). The emission decay traces were deconvoluted for the instrumental flash lamp by the Marquadt algorithm. For each measurement, at least five determinations were carried out.

(8) (a) Liu, H.-Q.; Cheung, T.-C.; Che, C.-M. *J. Chem. Soc., Chem. Commun.* **1996**, 1039. (b) Liu, H.-Q.; Cheung, T.-C.; Peng, S.-M.; Che, C.-M. *J. Chem. Soc., Chem. Commun.* **1995**, 1787. (c) Chan, C.-W.; Wong, W.-T.; Che, C.- M. *Inorg. Chem.* **1994**, *33*, 1266. (d) Chan, C.-W.; Lai, T.-F.; Che, C.-M.; Peng, S.-M. *J. Am. Chem. Soc.* **1993**, *115*, 11245.
(9) Constable, E. C.; Henney, R. P. G.; Leese, T. A.; Tocher, D. A. *J. Chem. Soc., Chem. Commun.* **1990**, 513.
(10) Cheung, T.-C.; Cheung, K.-K.; Peng, S.-M.; Che, C.-M. *J. Chem. Soc., Dalton Trans.* **1996**, 1645.
(11) (a) Maestri, M.; Deuschel-Cornioley, C.; von Zelewsky, A. *Coord. Chem. Rev.* **1991**, *111*, 117. (b) Maestri, M.; Balzani, V.; Deuschel-Cornioley, C.; von Zelewsky, A. *Adv. Photochem.* **1992**, *17*, 1 and references therein. (c) Carlson, G. A.; Djurovich, P. I.; Watts, R. J. *Inorg. Chem.* **1993**, *32*, 4483. (d) Spellane, P. J.; Watts, R. J.; Vogler, A. *Inorg. Chem.* **1993**, *32*, 5633. (e) Schmid, B.; Garces, F. O.; Watts, R. J. *Inorg. Chem.* **1994**, *33*, 9.
(12) Neve, F.; Ghedini, M.; Crispini, A. *Chem. Commun.* **1996**, 2463.
(13) Karash, M. S.; Seyler, R. C.; Mayo, F. R. *J. Am. Chem. Soc.* **1938**, *60*, 882.

Table 1. Crystal Data and Structure Refinement for **2**

empirical formula	$C_{34}H_{39}ClN_2OPt$
fw	722.2
temp	298 K
wavelength	0.71073 Å
crystal system	triclinic
space group	$P\bar{1}$
unit-cell dimens	$a = 9.043(2)$ Å
	$b = 10.874(2)$ Å
	$c = 15.710(4)$ Å
	$\alpha = 96.95(2)°$
	$\beta = 92.51(2)°$
	$\gamma = 102.32(2)°$
volume	1494.3(6) Å^3
Z	2
density (calcd)	1.605 g/cm^3
abs coeff	48.14 cm^{-1}
F(000)	720
scan type	$2\theta-\theta$
no. of independent reflns	5225 [R(int) = 0.017]
no. of obsd reflns [$I > 2\sigma(I)$]	4333
no. of parameters	352
final R indices[a,b]	$R = 0.0387$, $R' = 0.0335$
goodness-of-fit	1.50
largest and mean Δ/σ	0.001, 0.000

[a] $R = \sum||F_o| - |F_c||/\sum|F_o|$. [b] $R' = [\sum w(|F_o| - |F_c|)^2/\sum w|F_o|^2)^{1/2}$.

Luminescence quantum yields were obtained by using the optically dilute method[14] (quantum yield standards were $[Ru(bpy)_3]^{2+}$ in aerated aqueous solution ($\Phi = 0.028$[15]) for the visible emission and anthracene in degassed ethanol ($\Phi = 0.27$[16]) for the UV emission). Experimental errors were as follows: absorption and emission maxima, ±2nm; molar absorption coefficients, 10%; emission lifetimes, 10%; luminescence quantum yields, 20%.

^{1}H and ^{13}C NMR spectra were recorded on a Bruker AC300 spectrometer.

Crystal Structure Determination. Orange crystals of [Pt(L^1)Cl] (**2**) suitable for diffraction analysis were obtained from a chloroform/ethanol mixture. Diffraction measurements were carried out on a Siemens R3m/V automated four-circle diffractometer equipped with graphite-monochromated Mo Kα radiation ($\lambda = 0.710\ 73$ Å). The unit cell dimensions were obtained by application of the automatic diffractometer indexing routine to the positions of 33 reflections, with 2θ angles in the range 16−28°. The data were corrected for Lorentz, polarization, and X-ray absorption effects, and an empirical absorption correction was applied using a method based upon azimuthal (Ψ) scan data.[17] Details of crystal data collection are listed in Table 1. The structure was solved by Patterson and Fourier methods and refined by full-matrix least-squares procedures. The weighting scheme used in the last refinement cycle was $w^{-1} = \sigma^2|F_o| + q|F_c|^2$, with $q = 0.0001$. All the non-hydrogen atoms were refined anisotropically, and the hydrogen atoms were included as idealized atoms riding on the respective carbon atoms with C−H bond lengths appropriate to the carbon atom hybridization. The isotropic displacement parameter of each hydrogen atom was fixed at $U = 0.08$ Å^2. Convergence for 4333 observed reflections [$I > 2\sigma(I)$] and 352 parameters was reached at $R = 0.039$ and $R' = 0.034$ with a goodness of fit of 1.50. The final Fourier-difference map was featureless, with maximum positive and negative peaks of 1.43 (1.1 Å from the Pt atom) and −0.69 e Å^{-3}, respectively. All calculations were performed with SHELXTL PLUS[18] and PARST[19] programs. Atomic scattering factors were as implemented in the SHELXTL PLUS program.

Results and Discussion

The cyclometalating ligand HL^1 can be conveniently prepared through a typical Kröhnke[20] synthesis (Scheme 1). The reaction of the appropriate enone with *N*-phenacylpyridinium bromide in the presence of an excess of ammonium acetate resulted in the formation of a crude product. Purification by chromatography afforded the pure ligand in 43% yield.

The cyclometalated species [Pd(L^1)Cl] and [Pt(L^1)Cl] were then obtained by different standard methods, according to the different ease of metalation at Pd(II) and Pt(II) centers. A room-temperature reaction between HL^1 and $[Pd(PhCN)_2Cl_2]$ in benzene/methanol was sufficient to give [Pd(L^1)Cl] (**1**) as a pale green solid in high yield. Proton NMR spectroscopy confirmed the presence of a deprotonated HL^1 ligand. As cycloplatination often requires more drastic conditions, the cyclometalated [Pt(L^1)Cl] (**2**) was obtained only under reflux conditions by reaction of $K_2[PtCl_4]$ and HL^1 in acetonitrile/water/ethanol. This mixture of solvents was found to be preferable to aqueous acetonitrile, a medium commonly used for similar reactions of 6′-phenyl-2,2′-bipyridine (HL^2)[7d,10] and 6′-(2-thienyl)-2,2′-bipyridine (HL^3).[7c] This prevented the formation of a black solid in the early stage of the reaction. $[Pt(2\text{-Me-allyl})Cl]_2$ could not be used as a starting material for a cycloplatination to be carried out under milder conditions.[21] In fact, attempts to use $[Pt(2\text{-Me-allyl})Cl]_2$ to cyclometalate HL^1 only gave an unknown species that contained a "Pt(HL^1)" fragment with an N,N-coordination and which is not simply $[Pt(HL^1)Cl_2]$. Complex **2** formed directly from the the reaction mixture as a pure, orange solid. However, recrystallization gave two different forms, depending on the method used. Whereas rapid precipitation from a chloroform solution with diethyl ether gave **2** as a dark green solid, slow diffusion of ethanol through the chloroform solution gave well-formed, orange crystals of **2**. In both cases, solutions of the two forms have identical proton NMR spectra. A similar behavior has been previously observed by Constable for $[Pt(L^2)(MeCN)]PF_6$.[9]

The thermal behavior of complexes **1** and **2** was studied by differential scanning calorimetry (DSC) (rate of 10 °C min^{-1}) and optical microscopy. Both species have similar melting points, although **2** undergoes several endothermic crystal-to-crystal transitions before melting into a red-orange isotropic liquid. In addition, **2** shows an exothermic transition at about 158 °C, also visible from polarizing optical microscopy. The latter technique confirmed the absence of liquid crystalline phases.

X-ray Crystal Structure of [Pt(L^1)Cl] (2). The atomic coordinates and isotropic displacement coefficients, U(eq), are listed in Table 2. Table 3 lists relevant bond lengths and angles. A view of the structure of **2** is shown in Figure 1. Although already briefly reported,[12] the X-ray crystal structure of **1** will be recalled for comparison, where appropriate.

The Pt atom in **2** reveals a distorted square-planar geometry with the N(2)−Pt−C(2) angle of 161.4(3)° deviating from linearity. This type of distortion is common for Pt(II) square-planar centers bound to terdentate ligands that form two fused five-membered chelate rings.[8d,9,10,22,23] The corresponding angle for [Pd(L^1)Cl] (**1**) has been found to be 160.9(4)°.[12] The bond distances within the two chelate rings [PtNCCN and [PtCCCN]

(14) Demas, J. N.; Crosby, G. A. *J. Phys. Chem.* **1971**, *75*, 991.
(15) Nakamaru, K. *Bull. Chem. Soc. Jpn.* **1982**, *55*, 2697.
(16) Dawson, W. R.; Windsor, M. W. *J. Phys. Chem.* **1968**, *72*, 3251.
(17) North, A. C. T.; Phillips, D. C. *Acta Crystallogr., Sect. A* **1968**, *24*, 351.
(18) *SHELXTL PLUS*, Version 4.21; Siemens Analytical X-ray Instruments Inc.: Madison, WI, 1990.
(19) Nardelli, M. *Comput. Chem.* **1983**, *7*, 95.
(20) Kröhnke, F. *Synthesis* **1976**, 1.
(21) Pregosin, P. S.; Wombacher, F.; Albinati, A.; Lianza, F. *J. Organomet. Chem.* **1991**, *418*, 249.
(22) Yip, H.-K; Cheng, L.-K.; Cheung, K.-K.; Che, C.-M. *J. Chem. Soc., Dalton Trans.* **1993**, 2933.
(23) Minghetti, G.; Cinellu, M. A.; Stoccoro, S.; Zucca, A.; Manassero, M. *J. Chem. Soc., Dalton Trans.* **1995**, 777.

Table 2. Atomic Coordinates ($\times 10^4$) and Equivalent Isotropic Displacement Coefficients ($Å^2 \times 10^3$) for **2**

atom	*x*	*y*	*z*	*U*(eq)[a]
Pt	823(1)	3623(1)	4088(1)	47(1)
Cl	2916(2)	2915(2)	4533(1)	71(1)
N(1)	−891(6)	4249(5)	3679(3)	44(2)
N(2)	1793(5)	5588(5)	4175(3)	47(2)
O(1)	−8179(5)	6888(5)	1585(3)	77(2)
C(1)	−2153(7)	2097(6)	3594(4)	52(3)
C(2)	−681(7)	1978(6)	3905(4)	53(3)
C(3)	−573(8)	767(6)	4079(5)	59(3)
C(4)	−1809(8)	−234(7)	3970(5)	67(3)
C(5)	−3210(9)	−102(7)	3655(5)	75(3)
C(6)	−3391(8)	1072(7)	3458(5)	64(3)
C(7)	−2244(7)	3395(6)	3452(4)	49(2)
C(8)	−3465(7)	3811(6)	3131(4)	50(2)
C(9)	−3345(7)	5094(6)	3030(4)	46(2)
C(10)	−1950(7)	5916(6)	3285(4)	49(2)
C(11)	−755(7)	5486(6)	3600(4)	46(2)
C(12)	804(7)	6252(6)	3876(4)	47(2)
C(13)	1223(8)	7544(6)	3875(5)	56(3)
C(14)	2667(8)	8177(7)	4157(5)	65(3)
C(15)	3682(8)	7502(7)	4465(5)	62(3)
C(16)	3206(7)	6216(7)	4455(4)	53(3)
C(17)	−4644(7)	5527(6)	2648(4)	45(2)
C(18)	−6077(8)	4738(7)	2468(5)	60(3)
C(19)	−7275(7)	5145(7)	2102(4)	59(3)
C(20)	−7077(8)	6375(7)	1926(4)	58(3)
C(21)	−5674(9)	7174(7)	2098(5)	74(3)
C(22)	−4487(8)	6760(7)	2447(5)	63(3)
C(23)	−9638(7)	6123(7)	1311(5)	68(3)
C(24)	−10559(8)	7048(8)	1028(5)	80(4)
C(25)	−12120(8)	6425(8)	602(5)	76(4)
C(26)	−12975(8)	7401(8)	356(5)	82(4)
C(27)	−14542(8)	6883(9)	−84(5)	85(4)
C(28)	−15335(8)	7901(9)	−300(6)	90(4)
C(29)	−16938(9)	7443(9)	−712(5)	86(4)
C(30)	−17673(8)	8492(8)	−952(5)	81(4)
C(31)	−19284(8)	8050(8)	−1343(5)	74(3)
C(32)	−20025(8)	9105(8)	−1546(6)	81(4)
C(33)	−21630(8)	8669(8)	−1955(5)	78(4)
C(34)	−22326(10)	9763(8)	−2150(7)	120(5)

[a] Equivalent isotropic *U* defined as one-third of the trace of the orthogonalized $\mathbf{U}_{ij}$ tensor.

Table 3. Selected Bond Lengths and Angles for [Pt(L[1])Cl] (**2**)

Bond Distances (Å)			
Pt−Cl	2.302(2)	Pt−N(1)	1.935(5)
Pt−N(2)	2.115(5)	Pt−C(2)	1.984(6)
N(1)−C(7)	1.372(7)	N(1)−C(11)	1.345(8)
N(2)−C(12)	1.365(9)	C(1)−C(2)	1.434(10)
C(1)−C(7)	1.475(10)	C(11)−C(12)	1.493(8)

Bond Angles (deg)			
Cl−Pt−N(1)	177.8(2)	Cl−Pt−N(2)	99.6(1)
N(1)−Pt−N(2)	79.1(2)	Cl−Pt−C(2)	98.9(2)
N(1)−Pt−C(2)	82.4(2)	N(2)−Pt−C(2)	161.4(3)
Pt−N(1)−C(7)	118.4(4)	Pt−N(1)−C(11)	121.0(4)
Pt−N(2)−C(12)	112.4(3)	C(2)−C(1)−C(7)	114.5(5)
Pt−C(2)−C(1)	112.8(5)	N(1)−C(7)−C(1)	111.9(6)
N(1)−C(11)−C(12)	112.3(6)	N(2)−C(12)−C(11)	115.1(5)

are in good agreement with those reported for other platinum(II) 6′-phenyl-2,2′-bipyridine complexes[9,10] and are similar to those seen for **1**. Moreover, the presence of a short Pt−N bond length to the central pyridine ring [1.935(5) Å] and a longer one to the lateral pyridine ring [2.115(5) Å] is common to the platinum(II)−2,2′:6′,2″-terpyridine derivatives. The analysis of nine structures containing the 2,2′:6′,2″-terpyridine coordinated ligand recorded in the Cambridge Structural Database (CSD)[24] has given mean values of the Pt−N bonds as 1.93(2) and 2.02(2) Å, respectively. In our case, the longer Pt−N(2) distance also results from the strong *trans* influence of the phenyl carbon C(2).

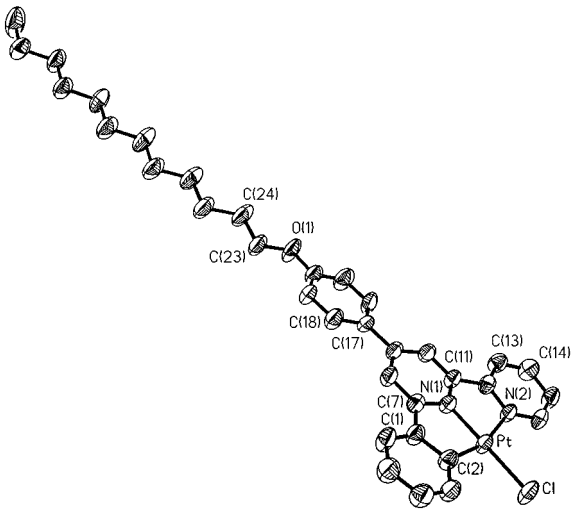

Figure 1. Molecular structure of [Pt(L[1])Cl] (**2**) showing the numbering scheme adopted. Thermal ellipsoids are depicted at the 50% probability level.

Both complexes **1** and **2** show essentially planar chelate rings. The maximum deviations from planarity are 0.007(8) Å [N(2) in [PdNCCN]] and 0.027(6) Å [C(12) in [PtNCCN]], respectively. The dihedral angles between the two five-membered rings are very similar (1.2(2)° in **1** and 1.3(2)° in **2**). For both complexes **1** and **2**, the whole coordinated portion of the ligand is planar, as proved by the dihedral angles between the central and the lateral aromatic rings [3.1(3) and 4.1(2)° for complex **1**; 4.2(2) and 1.1(2)° for complex **2**]. The rotationally free phenyl ring becomes coplanar with the rest of the aromatic system on going from complex **1** to complex **2**, with tilt angles of 21.5(1)° in the former case and 8.0(1)° in the latter. A further difference between the structures of **1** and **2** is related to the conformation of the peripheral hydrocarbon chain. While in **1** the dodecyloxy chain deviates strongly from an *all-anti* conformation [maximum deviation of 58(4)° about C(30)−C(31)[12]], in **2** it shows a regular *anti* conformation with mean torsion angle of 178(7)°.

The packing of complex **2** in the crystal is shown in Figure 2 (top view). The shortest Pt---Pt intermolecular separation of 4.426(1) Å occurs between centrosymmetrically related molecules, which are approximately superimposed along the *c* axis. The two molecules are slipped-stacked along the *a* axis, with a transverse slip around 4 Å. This is reminiscent of the molecular packing observed in complex **1**, where the shortest Pd---Pd contact is 5.667(2) Å.[12] In both cases, the two molecules superimpose in a head-to-tail orientation and the two square planes are twisted with respect to each other, with average torsion angles of 37.9° (complex **1**) and 37.0° (complex **2**). Although it is reasonable to exclude a metal−metal interaction in complex **2** (Pt---Pt > 4 Å), the existence of ligand $\pi-\pi$ interactions within the dimeric units is apparent from the intermolecular plane separation (3.42 Å) between the coordinated portions of the ligand. The stacked parts of the ligand are the cycloplatinated ring [PtCCCN] of one molecule and the lateral pyridine ring of the centrosymmetrically related molecule. The repetition of the dimeric unit along the *a* axis gives rise to the shortest interdimeric Pt---Pt separation of 7.787(2) Å. In addition, molecules of dimeric units show partial overlap between the rotationally free aromatic ring of one molecule and

(24) Allen, F. H.; Davies, J. E.; Galloy, J. J.; Johnson, O.; Kennard, O.; Macrae, C. F.; Mitchell, E. M.; Smith, J. M.; Watson, D. G. *J. Chem. Inf. Comput. Sci.* **1991**, *31*, 187.

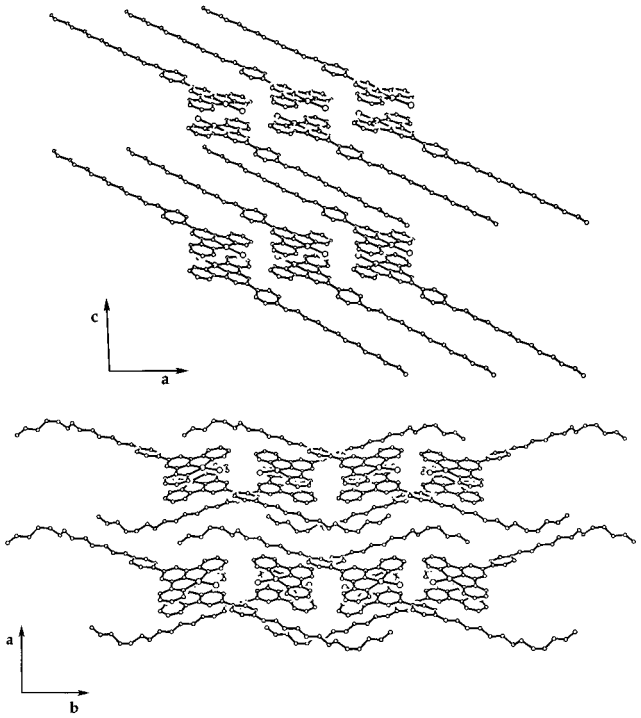

Figure 2. Crystal packing of [Pt(L[1])Cl] (**2**) (top view) and [Pd(L[1])Cl] (**1**) (bottom view).

the lateral pyridine ring of the other, with the shortest interatomic distance at 3.40(1) Å.

Finally, crystal packing shows that a compromise is at work between two different inherent tendencies of such complexes. Whereas the planar cores (that represent the polar, or at least polarizable, part of the molecules) roughly pile up along one direction, the nonpolar chains tend to confine themselves to a nonpolar region. This segregation effect is maximized for the platinum homologue **2**. Reasons for a somewhat different packing for **1** (Figure 2, bottom view) are to be found either in the different conformation of the hydrocarbon chain or in the reduced tendency of planar Pd(II) centers to stack.

Absorption Spectra and Photophysical Properties. The free protonated HL[1] ligand and its Pd(II) and Pt(II) complexes are fairly stable in CH_2Cl_2, as demonstrated by the constancy of their absorption spectra over 1 week.

The absorption spectrum of HL[1] (Figure S1 (Supporting Information)) is dominated by a strong band peaking at 295 nm ($\epsilon = 28\,480\ M^{-1}\ cm^{-1}$) followed at longer wavelengths by a weakly absorbing tail exhibiting a shoulder at about 360 nm ($\epsilon = 1030\ M^{-1}\ cm^{-1}$). The strong UV band is attributed to a $\pi \rightarrow \pi^*$ transition involving the aromatic framework, on the basis of the extinction coefficient and the similarity with the $\pi \rightarrow \pi^*$ band reported for other polypyridine complexes.[11,25] The tail at lower energy is assigned to n $\rightarrow \pi^*$ transitions, probably involving pyridine nitrogens and the alkoxy fragment.

The absorption spectrum of complex **2** (Figure 3, Table S5 (Supporting Information)) shows a moderately intense visible absorption feature ($\lambda_{max} = 420$ nm ; $\epsilon = 5400\ M^{-1}\ cm^{-1}$) which can be safely assigned to a metal-to-ligand charge-transfer (MLCT) transition from the dπ metal orbitals to a π^* orbital of the polypyridine ligand, by similitude with Pt(II)−terpypyridine[26] and cyclometalated[11] compounds, and intense absorption bands in the UV region. The latter bands are attributable to

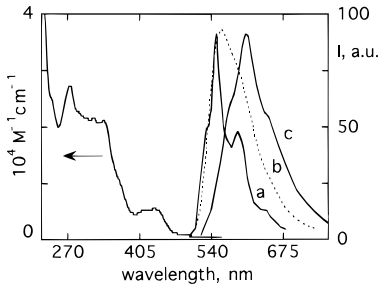

Figure 3. Absorption spectrum (on the left) of [Pt(L[1])Cl] in dichloromethane solution at room temperature and luminescence spectra of the same complex in butyronitrile rigid matrix at 77 K (a), in dichloromethane fluid solution at 298 K (b, dotted line), and in the solid state at 298 K (c). The luminescence spectra shown here are not corrected for photomultiplier response. Corrected values are given in the text.

metal-perturbed ligand-centered (LC) transitions. Complex **1** does not exhibit (Figure 4) a MLCT band in the visible region, as expected because the palladium(II) center is much more difficult to oxidize than the platinum(II) center. Therefore, MLCT transitions should occur at higher energy in **1** than in the platinum complex and probably contribute to the strong absorption at about 320 nm ($\epsilon = 15\,690\ M^{-1}\ cm^{-1}$), overlapping with the usual LC bands. In the absorption spectra of both complexes, a weak shoulder is present at about 365 nm. The fact that the energy of such a shoulder is unaffected on going from palladium to platinum complexes rules out metal-centered (MC) and MLCT attributions. This absorption feature is reminescent of the shoulder at 360 nm which is present in the spectrum of the protonated ligand, so that we have tentatively assigned it to n $\rightarrow \pi^*$ transitions involving the oxygen of the alkoxy group, which is far away from the chelation sites and is practically unperturbed by metal coordination.

The protonated ligand HL[1] exhibits strong UV luminescence when excited in the $\pi-\pi^*$ absorption band (see Figure S1; highest energy feature of the emission spectrum 350 nm; luminescence lifetime 1.6 ns; quantum yield 0.18). Because of the energy, lifetime, and quantum yield, the luminescence is assigned to the singlet $\pi \rightarrow \pi^*$ excited state. On excitation of the absorption tail at wavelengths longer than 380 nm, another very weak, broad, and unstructured luminescence band peaking at 500 nm can be seen ($\Phi < 10^{-4}$; excitation wavelength 390 nm). This band is tentatively assigned to the alkoxyphenyl moiety, suggesting that in the protonated free ligand this chromophore is essentially uncoupled with the phenyl−bipyridine framework, in which the $\pi \rightarrow \pi^*$ fluorescence originates.

Photophysical properties of platinum(II)− and palladium(II)−polypyridine complexes have been extensively studied.[27] The lack of room-temperature luminescence in fluid solution for many Pd(II) and Pt(II) complexes is usually due to the presence of low-lying MC excited states, which can be easily populated by thermal activation and provide fast deactivation pathways *via* molecular distortion.[11] The situation is quite different in a rigid matrix at 77 K. Under these conditions, the thermally-activated deactivation processes are blocked and luminescence from MLCT and/or LC levels can be obtained.[11] Besides the MLCT and LC excited states, d$\sigma^* \rightarrow \pi^*$(polypyridine) charge-

(25) Lytle, F. E.; Hercules, D. M. *J. Am. Chem. Soc.* **1969**, *91*, 253.
(26) (a) Aldridge, T. K.; Stacy, E. M.; McMillin, D. R. *Inorg. Chem.* **1994**, *33*, 722. (b) Bailey, J. A.; Hill, M. G.; Marsch, R. E.; Miskowski, V. M.; Schaefer, W. P.; Gray, H. B. *Inorg. Chem.* **1995**, *34*, 4591.
(27) For some representative examples, see refs 8, 10, 11, 26, and 28.
(28) (a) Sandrini, D.; Maestri, M.; Balzani, V.; Chassot, A.; von Zelewsky, A. *J. Am. Chem. Soc.* **1987**, *109*, 7720. (b) Kunkely, H.; Vogler, A. *J. Am. Chem. Soc.* **1990**, *112*, 5625. (c) Blanton, C. B.; Rillema, D. P. *Inorg. Chim. Acta* **1990**, *168*, 145. (d) Cummings, S. D.; Eisenberg, R. *Inorg. Chem.* **1995**, *34*, 2007. (e) Rosace, G.; Giuffrida, G.; Saitta, M.; Guglielmo, G.; Campagna, S.; Lanza, S. *Inorg. Chem.* **1996**, *35*, 6816.

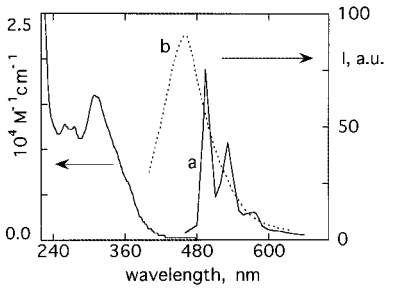

Figure 4. Absorption spectrum (on the left) of [Pd(L^1)Cl] in dichloromethane solution at room temperature and luminescence spectra of the same complex in butyronitrile rigid matrix at 77 K (a) and in the solid state at 298 K (b). The luminescence spectra shown here are not corrected for photomultiplier response. Corrected values are given in the text.

transfer (hereafter MMLCT) excited states have to be taken into account in d^8 square planar compounds. These excited states originate from metal−metal interactions usually occurring in stacked dimers (or polymers).[29] They are typical of solid-state systems and have been demonstrated to be responsible for the emission of a number of metal−metal-bonded systems.[29] Furthermore, when face-to-face oligomerization between Pt(II) or Pd(II) complexes carrying large aromatic frameworks leads to suitable arrangements, even excimeric emission can occur.[10,26b,28b] Oligomer formation, and the corresponding MMLCT and/or excimeric emission, is not limited to solid or glassy systems but is also found in fluid solution,[28b] and can give useful information about the extent of intermolecular interactions between the individual molecules, topics which are of basic importance for a number of interesting properties of the compounds, including liquid crystal behavior.

Complex **1** shows strong emission (highest energy feature 495 nm; $\tau = 74$ μs) in a butyronitrile rigid matrix at 77 K (Table S5, Figure 4). The 77 K glass emission spectrum is highly structured, exhibiting a vibronic progression of about 1300 cm^{-1} typical of C−N and C−C aromatic stretchings, and it can be essentially attributed to a ^{3}LC excited state partially mixed with a closely-lying ^{3}MLCT level, on the basis of the spectral shape and lifetime.[11,30] The luminescence is totally quenched in fluid solution at room temperature, as usual for Pd(II)−polypyridine complexes, because of the presence of low-lying, thermally-activated ^{3}MC states.[11,28] Room-temperature luminescence is also exhibited by microcrystalline samples of **1** ($\lambda_{max} = 490$ nm). Although the emission spectrum is unstructured (Figure 4), we assign this emission to the same ^{3}LC level responsible for the 77 K glassy emission, essentially because it occurs at a similar energy.

Complex **2** exhibits emission both at room temperature in dichloromethane fluid solution ($\lambda_{max} = 590$ nm; $\tau = 700$ ns; $\Phi = 0.037$) and at 77 K in butyronitrile glasses ($\lambda_{max} = 545$ nm; $\tau = 18$ μs; see Table S5 and Figure 3). The emission spectrum at 77 K is structured, and the vibrational progression is typical of luminescence originating from either ^{3}MLCT or ^{3}LC levels.[11,30] The emission spectrum at room temperature in fluid solution is slightly displaced to the red with respect to the 77 K emission, and the structure is almost totally lost. Because of the luminescence lifetimes and of the rate constant of the radiative transition ($k_r = 5.3 \times 10^4$ s^{-1}), obtained from room-temperature τ and Φ values, the emission of [Pt(L^1)Cl] is attributed to ^{3}MLCT level(s),[30] both in glassy matrix at 77 K and in fluid solution at room temperature. The excitation spectrum of **2** closely matches the corresponding absorption spectrum. In particular, even the shoulder at about 365 nm, assigned to the transition within the alkoxyphenyl chromophore (see above), contributes to the excitation spectrum, so indicating that excitation in the latter chromophore also results in population of the luminescent ^{3}MLCT level. This contrasts with the double emission exhibited by the HL^1 free ligand, suggesting that, in the platinum(II) complex, coupling between the alkoxyphenyl-centered excited state and the triplet MLCT state occurs.

It is now interesting to compare the photophysical properties of [Pt(L^1)Cl] (**2**) with those reported for the related cyclometalated complex [Pt(L^2)Cl] (as previously stated, HL^2 = 6′-phenyl-2,2′-bipyridine),[10] which is also luminescent from a ^{3}MLCT excited state both in fluid solution at room temperature and in glass at 77 K. The luminescent MLCT state of [Pt(L^1)Cl] is displaced toward the red with respect to the luminescent MLCT state of [Pt(L^2)Cl] (compare the 590 nm emission maximum of [Pt(L^1)Cl] with the 565 nm emission maximum of [Pt(L^2)Cl] in dichloromethane fluid solution and the 545 nm highest energy emission feature of [Pt(L^1)Cl] in butyronitrile at 77 K and the 515 nm highest energy emission feature of [Pt(L^2)Cl] in acetonitrile at 77 K). Such an energy difference can be attributed to the presence of an additional phenyl ring in L^1. The longer luminescence lifetime and higher quantum yield of the room-temperature emission of [Pt(L^1)Cl] compared with those for [Pt(L^2)Cl] (0.70 μs and 0.037 *vs* 0.51 μs and 0.025 for luminescence lifetimes and quantum yields of [Pt(L^1)Cl] and [Pt(L^2)Cl],[10] respectively) can be attributed to the increased energy difference in [Pt(L^1)Cl] between the luminescent ^{3}MLCT level and an upper-lying ^{3}MC excited state, which is held responsible for the dominant radiationless deactivation pathway of the luminescent level. Indeed, the lowest ^{3}MC levels of [Pt(L^1)Cl] and [Pt(L^2)Cl] should lie at practically the same energy.

A further interesting difference between the photophysical properties of [Pt(L^1)Cl] and [Pt(L^2)Cl] concerns their luminescence behavior in the solid state. In fact, the solid state emission of [Pt(L^2)Cl] measured at room temperature ($\lambda_{max} = 665$ nm) is substantially lower in energy than the emission of the complex at 77 K in a glassy matrix and at room temperature in fluid solution. This emission was assigned to a ^{3}MMLCT excited state,[10] in line with the crystal structure of the complex, which shows an intermolecular Pt−Pt separation of 3.28 Å, sufficient for inducing strong metal−metal interactions. On the contrary, the emission of [Pt(L^1)Cl] in the solid state at room temperature (highest energy feature at 590 nm, Figure 4) is quite similar in energy to the emission recorded in fluid solution, so that a ^{3}MLCT origin is proposed. The presence of a vibrational progression in the solid state emission strongly supports such an assignment.

The absence of any trace of MMLCT as well as of excimeric emission in [Pt(L^1)Cl] (**2**) indicates that axial metal−metal interactions and $\pi-\pi$ aromatic interactions between the polypyridine frameworks are not strong enough to affect the photophysical properties of the "isolated" molecules in both fluid solution and glasses. Although the situation can obviously be different in the fluid and glassy states, metal−metal distances are not expected to decrease and $\pi-\pi$ interactions are not expected to be enhanced. Furthermore, the absence of the above type of emission even in the solid state is in fair agreement with the crystal structure of the complex, which shows a Pt−Pt separation exceeding 4 Å and a head-to-tail arrangements of the complex molecules in the crystal packing. The Pt−Pt

(29) (a) Rounhill, D. M.; Gray, H. B.; Che, C.-M. *Acc. Chem. Res.* **1989**, *22*, 55. (b) Houlding, V. H.; Miskowski, V. M. *Inorg. Chem.* **1991**, *30*, 4446. (c) Nocera, D. G. *Acc. Chem. Res.* **1995**, *28*, 209. (d) Hill, M. G.; Bailey, J. A.; Miskowski, V. M.; Gray, H. B. *Inorg. Chem.* **1996**, *35*, 4585.
(30) Crosby, G. A. *Acc. Chem. Res.* **1975**, *8*, 231.

separation is too large to allow significant axial metal−metal interaction from spectroscopic and photophysical viewpoints, and $\pi-\pi$ interactions between polypyridine moieties are not effective as a consequence of the unfavorable arrangement of the molecules within the crystal.

Conclusions

We have shown that metalation of the HL^1 ligand effectively promotes lamellar or pseudolamellar crystal packing, depending on the nature of the metal ion. Yet the strong anisometry of the complexes is not sufficient to generate mesomorphism, as the factors that control the stability of the crystal phase are of increased importance.

Whereas the desired liquid-crystalline behavior failed to appear, photophysical studies have revealed interesting aspects, confirming the attractiveness of cyclometalated[10,11,31] and polypyridine[32] Pd(II) and Pt(II) species from a photophysical viewpoint. In fact, both **1** and **2** exhibit luminescence, although under different conditions. This study correlates the solid state properties of the cyclometalated complexes with the photophysical behavior. It is apparent that the introduction of long-chain alkoxy substituents in the periphery of the ligand leads to a reduced tendency toward metal−metal and interplanar stacking. This is reflected in luminescence properties significantly different from those of analogous species.

Acknowledgment. Financial support from the italian Ministero dell'Università e della Ricerca Scientifica e Tecnologica (MURST) and Consiglio Nazionale delle Ricerche (CNR) is gratefully acknowledged.

Supporting Information Available: Full tables listing atomic coordinates for hydrogens, complete bond lenghts and angles, and anisotropic thermal parameters for compound **2** (Tables S1−S4), absorption and emission spectra for the HL^1 ligand (Figure S1), and a listing of photophysical data for the complexes (Table S5) (6 pages). Ordering information is given on any current masthead page.

IC9703540

(31) (a) Mdleleni, M. M.; Bridgewater, J. S.; Watts, R. J.; Ford, P. C. *Inorg. Chem.* **1995**, *34*, 2334. (b) Craig, C. A.; Watts, R. J. *Inorg. Chem.* **1989**, *28*, 309.

(32) For recent examples, see: (a) Kato, M.; Sasano, K.; Kosuge, C.; Yamazaki, M.; Yano, S.; Kimura, M. *Inorg. Chem.* **1996**, *35*, 116. (b) Connick, W. B.; Henling, L. M.; Marsh, R. E.; Gray, H. B. *Inorg. Chem.* **1996**, *35*, 6261.